SPATIAL ASSESSMENT OF LAND SURFACE TEMPERATURE AND EMISSIVITY IN THE TROPICAL LITTORAL CITY OF PORT HARCOURT, NIGERIA

Abstract

The study examined Land Surface Temperature (LST) and Land Surface Emissivity (LSE) in a tropical coastal city of Port Harcourt and its environs. Satellite remote sensing of multiple-wavelength origin was employed to derive data from the Landsat Enhance Thematic Mapper (ETM+). Statistical mean and range were used to show pattern of LST and LSE. The study established the relationship and characteristics of land use land cover, built-up area and influence of population on land surfaces. With population of over 3,095,342 persons occupying surface area of approximately 458,28Km^2, rapid vegetal and water body lost have put the city area under pressure of 4.7^{0}C heat bias at the interval of 15 years. From rural fringes to the city center, LST varies with 9.3^{0}C in wet season and 4.8^{0}C in the dry season. During the dry season, LSE is severe in the southern part of the city contributed by water bodies, more vegetal cover and urban pavement materials. Emissivity in the wet season varied with 0.0136 and 0.0006 during the dry season but differs with 0.0165 between the two seasons. One critical finding is that LSE decreases from the rural fringes to the city center and LST increases from the rural fringes to the city center. It is recommended that urban greening at the city center should be practiced and the rural fringes should be explored by decongesting activities at the city center to the outskirts in order to ameliorate the effects of urban heat bias without further delay.

Keywords: Port Harcourt; Land Use Type; Land Surface Temperature; Land Surface Emissivity

1.0 INTRODUCTION

It is considered that temperature of cities in the world has gradually risen due to urbanization with population explosion. In the process of urbanization, the biophysical features of the city are altered. Thus, many factors have caused this alteration such as emission of greenhouse gas, increased pavement surfaces, loss of urban tree cover, urban morphology and low albedo of materials [1]; others are thermal properties of materials, city size and generated anthropogenic heat [2]. When city temperature is compromised, there will be noticeable increased energy consumption, high emissions of air pollutants and greenhouse gases, conceded human health and comfort as well as impaired water quality [3]. In an urban area, a greater part is occupied with manmade pavement materials and structures which change the thermal properties of the surface areas facilitated by asphalt, cement concrete and other structures that have fast heat absorption. As a result, the pavement surface temperature is distinctively higher than the natural surfaces across the different land use types resulting to the phenomenon of Urban Heat Island (UHI) [4].

Conventionally, researchers investigate temperature characteristics in the city using the known air temperature readings from thermometers located at various land use types in the city area [5]. [6] introduced the

chance of using satellite images in studying thermal sources and effects generated by urban pavement materials and their distribution in the urban space. Thus, Satellite Remote Sensing (SRS) has been extensively useful and recommended as an effective tool in the study of urban land use, Land Surface Temperature (LST) and Land Surface Emissivity (LSE) as well as heat island characteristics. SRS gathers multispectral, multi-resolution and multi-temporal data and converts them to information valued for monitoring and understanding urban land processes and the associated heat fluxes [7]. Many Thermal Infrared Images (TII) of varied resolutions have been applied in carrying out investigation of LST and LSE such as the Advance Space Born Thermal Emission and Reflection Radiometer (ASTER), Moderate Resolution Imaging Spectroradiometer (MODIS), Enhanced Thematic Mapper (ETP+) [8] [9].

LST is the degree of hotness a given surface of the earth would be when touched. It is the temperature recorded by a satellite pass on a particular land surface when viewed from above [10]. The view could be buildings, grassland, roofs, water bodies, asphalt roads and the general urban concrete materials. LST has been recognized to spread across the urban surface areas. For instance [11] in China, Beijing noted temperature variation across different land use types using RS with the center bearing the highest temperature intensity of 24.1 ^{0}C. LSE is the proportion of radiated energy on the surface of a material compared to that released from a black body all at the same temperature, wavelength and conditions of view [12]. LSE determines the efficacy of urban surface areas to convert sensible heat into latent heat. It is the radiation of solar energy from material surface area to the surrounding air [13]. In the city and its environment exist strong relationship between the various land surfaces and LST as well as LSE characterized by the alteration of the biophysical features influenced by prevailing seasonal conditions in the area [14]. Therefore, this study examined spatial variation of LST and LSE in a coastal City of Port Harcourt, Nigeria.

2. Materials and Method

2.1 Description of Study Location

Port Harcourt City and Environs is in the South-South zone and Niger Delta area of Nigeria located within Latitudes 4^{o}05’30’’N and 5^{o}14’25’’N and Longitudes 5^{o}40’30’’E and 7^{o}11’01’’E of the Greenwich Meridian (GM). The two principal local government areas are Obio/Akpor and Port Harcourt City. Port Harcourt and environs extend to the fringes of Etche, Okirika, Degema Ikwere, Eleme, Emohua and Oyibo LGAs respectively (Figures 1). The area is located within the Niger Delta coastal zone made up of sedimentary formations. As a coastal city, the equatorial monsoon climate influences its atmospheric characteristics due to its nearness to the Atlantic Ocean. Both the maritime and continental air masses control the rainfall and temperature pattern of the city [15]. Also, as a city located within the Inter-Tropical Convergence Zone (ITCZ) in the African continent, it is affected with the warm humid maritime tropical air mass with its south-western winds and the hot and dry continental air mass from the north-easterly winds. The moist south-west wind in the area generates heavy rainfall volumes ranging from 2000mm to 2500mm with the peak period from April to September and in some years extends to October [16]. From April, relative humidity increases, peaking in July to September and dropping steadily and continuously till March with the lowest trough in January [17]. In a year cycle, temperature peaks in January to March and relative humidity drops

continuously within the months. The urban heat island that affects human comfort is a function of air temperature during dry season, relative humidity during the wet season and wind flow systems in the dry season [18]. Average peak temperature is 32°C and the lowest 26°C are usually observed in January and July respectively [19]. The humidity is high with mean annual figure at 85% with high and low peaks during the wet and dry seasons respectively [20]. Cloud cover pattern in the area is continuously improved with monthly average of over 6 Oktas [19] due to the massive water vapor that rises to the atmosphere as a result of adjacent water bodies. Cloud cover is highest during the wet season and lowest during the dry months respectively. The average daily sunshine was less than 3 hours as observed in July and about 4-5 hours in January and December respectively [21]. For the wind speed pattern, mean monthly range is between 0-3m/s [16] with high and low trends observed during the nocturnal hours. Urban heat island is influence by these climatic parameters operating in Port Harcourt Metropolis and Environs, Rivers State, Nigeria.

Fig 1 Port Harcourt City and Environs

2.2 Data and Methodology

Both descriptive and analytical approaches were employed for the investigation. Population model was used to estimate heat bias in 2001 and 2017 in relation to satellite imageries of land use land cover of the years. The study utilized RSS in the form of Normalized Difference Vegetation Index (NDVI), Normalized Difference Built-up Index (NDBI), LST and LSE retrieved during the dry season (January, 2017) and Wet season (August, 2017) as in Table 1: The parameters include: temperature profile, emissivity profile, land cover classification and land use/built-

up classification. They were derived from Landsat Enhanced Thematic Mapper (ETM+) and analyzed. In this process [22], Digital Number (DN) of the satellite origin was converted to Spectral Radiance (SR) where SR was converted to at-Sensor Temperature and Emissivity. Finally, surface emissivity was used to evaluation the land surface temperature from brightness temperature known as the LST value in the thermal band image as in Figure 2.

Table 1: Details of Landsat data Retrieved

Dates of Retrieval	Satellite/Sensor	Reference System/Path/Row
01/06/17 - 03/12/17	Landsat 8/ETM	LC08/L1TP/188057
08/18/17 - 08/26/17	Landsat 8/ETM	LC08/L1TP/188057

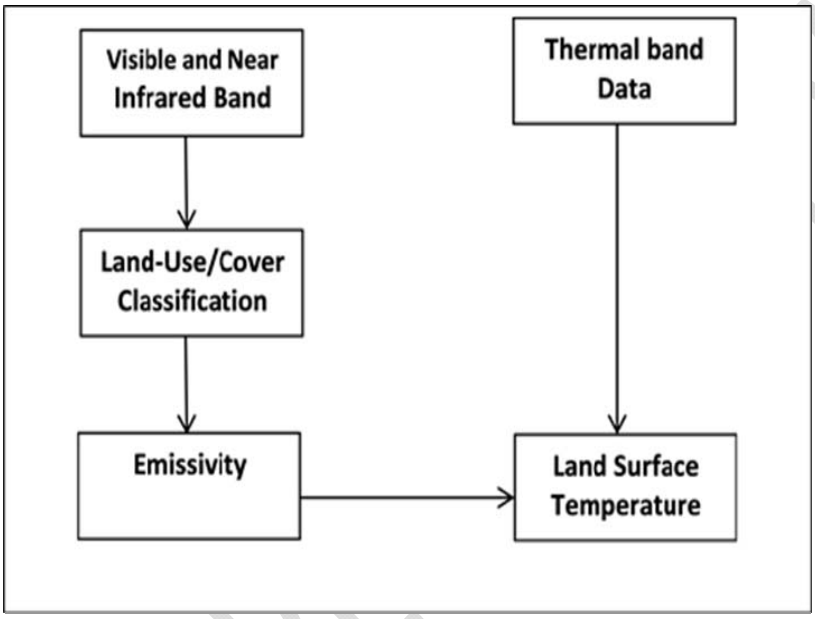

Fig 2 Data Processing Flow. Source: Qin, 2001

In the process of the satellite data analysis, it was Landsat 8, band 10 and 11 data that were used to estimate the LST and LSE. Thus, the Landsat imageries were imported to the GIS environment where analysis was carried out on the imageries. The following formulas were used for the Normalized Difference Vegetation Index (NDVI):

NDVI = (NIR-RED) / (NIR+RED) ---------- (1)

The RED and NIR are the spectral reflectance measurements acquired in the red (visible) and near-infrared regions which were represented with the values between 0.0 and 1.0; this formula yields a value that ranges from -1 (usually water) to +1 (strongest vegetative growth) respectively. Also, the Normalized Difference Built-up Index (NDVI) was carried out with the formula as follows:

NDBI = (SWIR-NIR) / (SWIR + NIR) ---------- (2)

The Sun elevation value = 51.8851 and the Sin (sun elevation) = 0.7867748

The raster calculator was used to derive the output data for RED reflective for the Red band to show the reflectance value within the band, NIR reflectance and finally the SWIR reflectance. The digital numbers of the imageries were converted to radiance using the formula thus:

$L\lambda$ = MLQ cal + AL ---------- (3)

Where Lλ is the TOA (Top of Atmosphere) spectra radiance (watts/ (m2 x srad x μm)), ML is the Band specific multiplicative rescaling factor from the metadata (Radiance multi band x, where x is the band number), AL represents the Band specific additive rescaling factor from the metadata (Radiance add band x, where x is the band number), Cal is the Quantized and calibrated standard product pixel value (DN). The Spectral radiance was converted to satellite brightness temperature using the thermal constant provided in the metadata. The formula is as follows:

$T = K_2/(K_1/LA+1)$ ---------- (4)

Where T is the At satellite surface temperature (K), LA is TOA Spectral radiance (watt/(m_2x Band x μm)), K_1 denotes the Band specific thermal conversion constant from metadata (k_1 Constant Band x, where x is the band number 10 or 11), K_2 is the Band specific thermal conversion constant from the metadata, (k_2 Constant Band x, where x is the band number 10 or 11). They were derived in degree kelvin which was converted to degree Celsius using the 272.15 conversion factor. The land surface temperature was thereafter calculated using the formula:

$BT/1+w \times (BT/P) \times \ln(\varepsilon))$ ---------- (5)

Where BT is the At satellite temperature, W is the Wavelengths of emitted radiance (11.5μm), P was derived from h x c/s (1.438×10^n – μmk), h was taken from Plank's constant (6.626×10^n – 23J/k), S represents Boltmann Constant (1.38×10^{-23} J/k), c as the Velocity of light (2.998×10^8 m/s) and ε equals to 14380.Land surface emissivity was calculated with e = 0.004pv + 0.986. Also Pu denotes proportion of vegetation according to the equation below:

$Pu = MDUI – MDUI_{min}/MDUI_{max} - MDUI_{min})^2$ ---------- (6)

Landsat imageries of 2001 (ETM+) and 2016 (ETM+) were employed to observe the differences in land cover and the infrastructural built-up area. The indices for the alteration of the biophysical land surfaces were the Normalized Difference Vegetation Index (NDVI) and Normalized Difference Built-up Index (NDBI) Landsat imageries. The NDVI was applied to differentiate the greenness of the area and the NDBI was employed to distinguish the built-up of the area in terms of infrastructure and pavement material differences.

3. RESULTS AND DISCUSSION

3.1 LAND USE LAND COVER, POPULATION AND HEAT BIAS

Globally, urbanization is increasing with population rise. Urban surfaces are progressively altered and biophysical features are lost resulting to heat stress. Therefore, it is necessary to relate the level of population, heat

bias and extent of city expansion as they contribute to LST and LSE between 2001 and 2017 (16 years interval). Population prediction model and heat stress according to [23] is important in the study of urban area climate forecast and planning as a mitigation measure to man's modification of the biophysical environment with the formula:

$$UHI = 0.73 \log_{10} Pop$$

Where: Pop equals to population.

Population of the nine Local Government Areas (LGAs) of Port Harcourt and environs (Obio/Akpor, Port Harcourt City, Oyibo, Okirika, Ikwere, Etche, Eleme, Emohua and Degema LGAs) has projected value of 3,229,384 persons [24] as in Figure 3.

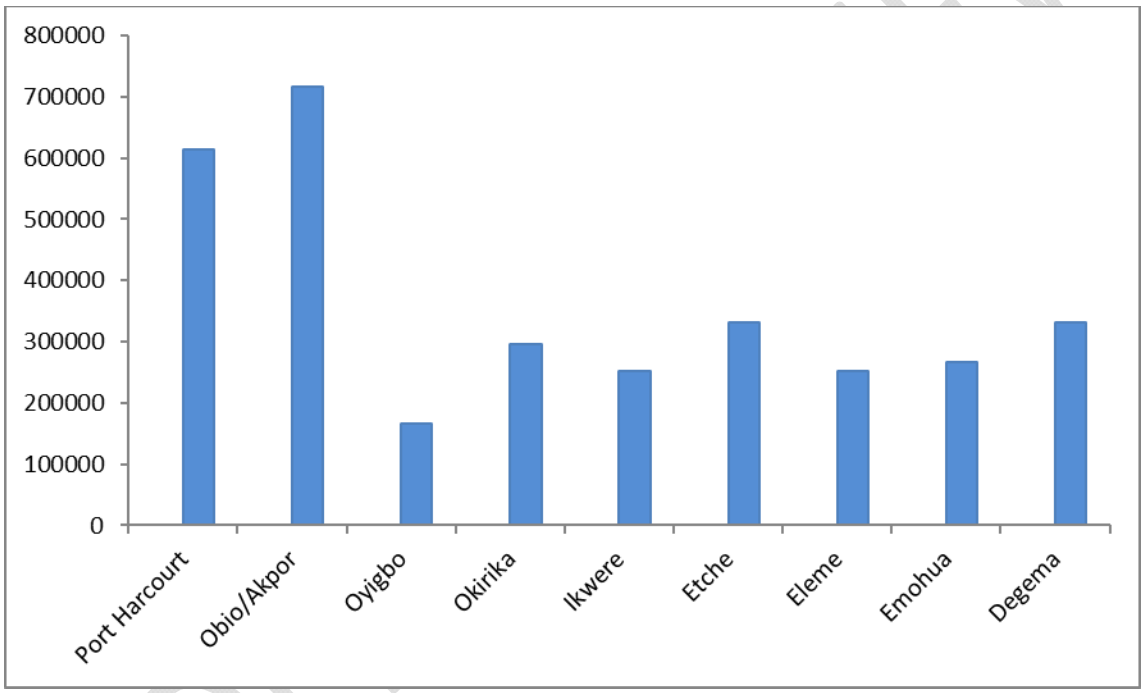

Fig 3: Population of Port Harcourt City and Surrounding LGAs.

Table 2: Projected Population and Heat Bias of Port Harcourt Area

Year	**2001**	**2016**	**2017**
Population	2,029,733	3,095,342	3,166,373
Heat Bias	4.6	4.7	4.7

The urban heat bias is a product of LST and LSE resulting from changes in population of people carrying out various anthropogenic activities of urban infrastructural development and expansion. In 2001(Figure 4), there was relatively dense vegetal cover, water bodies and other biophysical features with a population of 2,029,733 persons and heat bias of 4.6^0C (Table 2). In the same period, there was relatively limited modification of the biophysical features of the city surfaces with high coverage of primary and secondary forests as well as built-up

171 infrastructures especially in the northern segment of the city compared to 2016 land cover (Figure 5) with a
172 population of 3,095,342 persons and heat bias of 4.7^{o}C. Within the interval of 15 years, with population difference
173 of 1,065,609 persons, the heat bias in the city and its environs recorded 0.1^{o}C variation which seems to be
174 contributed by urban surface fluxes and material radiation. In this period, the southern coast of the city was
175 dominated with swamp forests and water bodies which inhibited built-up infrastructures and other manmade
176 materials. However, in 2016 (15 years later) Port Harcourt city and environs (Figure 6) experienced intensive built-
177 up area with limited swap forests altered by urbanization processes. Primary forests severely disappeared replaced
178 by secondary forests extending to all parts of the city surface areas. Built-up surfaces were observed spreading
179 toward the northern part such as Choba, Eliozu, Elelenwo as well as the extension to Trailer Park area. This is in
180 tandem with the findings of [25] in a land study of Port Harcourt environment covers surface area of 458.28Km^2
181 with population rise of 71,040 persons per annum and increased built-up area of 8,86Km^2 in each year. In the period
182 of the study, vegetal lost was 2.84Km^2 per annum, water body lost was 7.68Km^2 and farmland/secondary vegetation
183 increased by 2.35Km^2 [25].

184 In 2017, land use types in Port Harcourt city and environs was made up of high residential, medium
185 residential, residential/commercial, low residential, recreational, military, commercial, educational,
186 administrative/industrial, roads as well as other human activities (Table 3) with a population of 3,166,373 persons
187 and heat bias of 4.7^{0}C. At the city center, there were high and medium residential settlements capable of inducing
188 LST and LSE. On the other hand, there were more medium residential areas as one shift away from the city center.
189 Also, there were noticeable high residential settlements dispersed across the land use types (Figure 6). Recreational
190 and low residential land use types were physically scanty due to poor greening and increased urban pavement
191 materials. High population of Port Harcourt city and environs has resulted to having scanty low residential areas
192 especially the northern part of the city where there is rapid urban growth. The north-western part of the city has
193 more asphalt roads capable of increasing solar radiation from surfaces. The mixed pattern of manmade pavement
194 materials and other biophysical features are capable of generating varied radiation and emissivity across the different
195 land use types.

196 Normalized Difference Vegetation Index (NDVI) in the imageries display areas with high vegetal cover
197 such as grass land; forests show gray color and areas with low built-up and pavement materials appear blue and high
198 built-up showed pink color. The NDBI during the wet season (Figure 7) was high at the city center, north and north-

199 eastern part. NDBI in the wet season varied with 1.346 from the highest dense area to the less dense area. NDBI was
200 very low at the extreme south and south-western section of the city environment. On the other hand, NDBI in the
201 dry season (Figure 8) had similar spread with the wet season but with scattered spots at the south-western part of the
202 city and its rural outskirts. Both seasons had NDBI variation of 0.336. Low NDBI in the southern part of the city is
203 suspected to be limited by loss of buildings and other urban infrastructures due to coastal flooding.

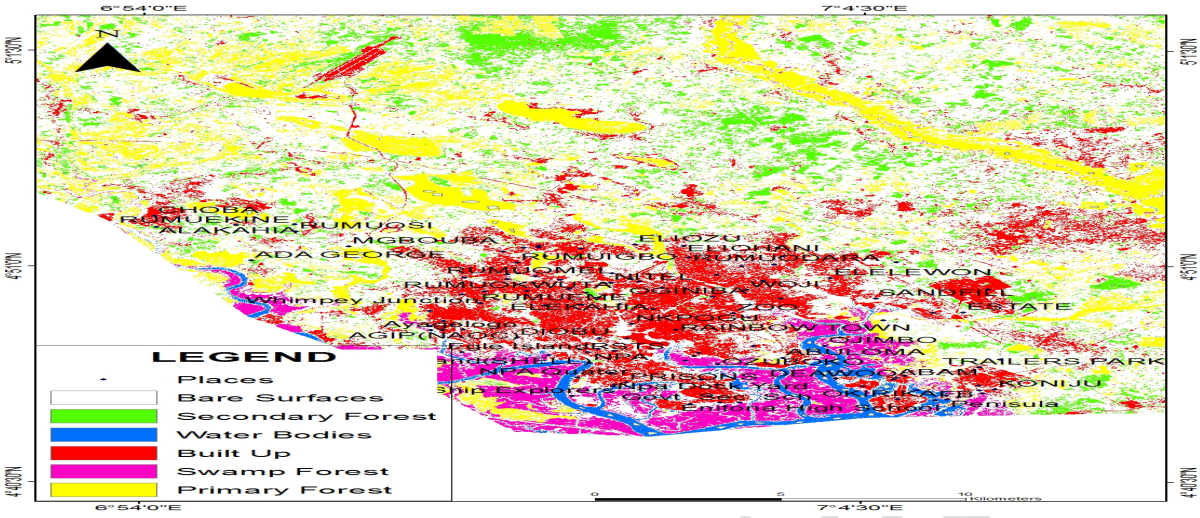

Fig 4 Land Cover of Port Harcourt City and Environs, 2001

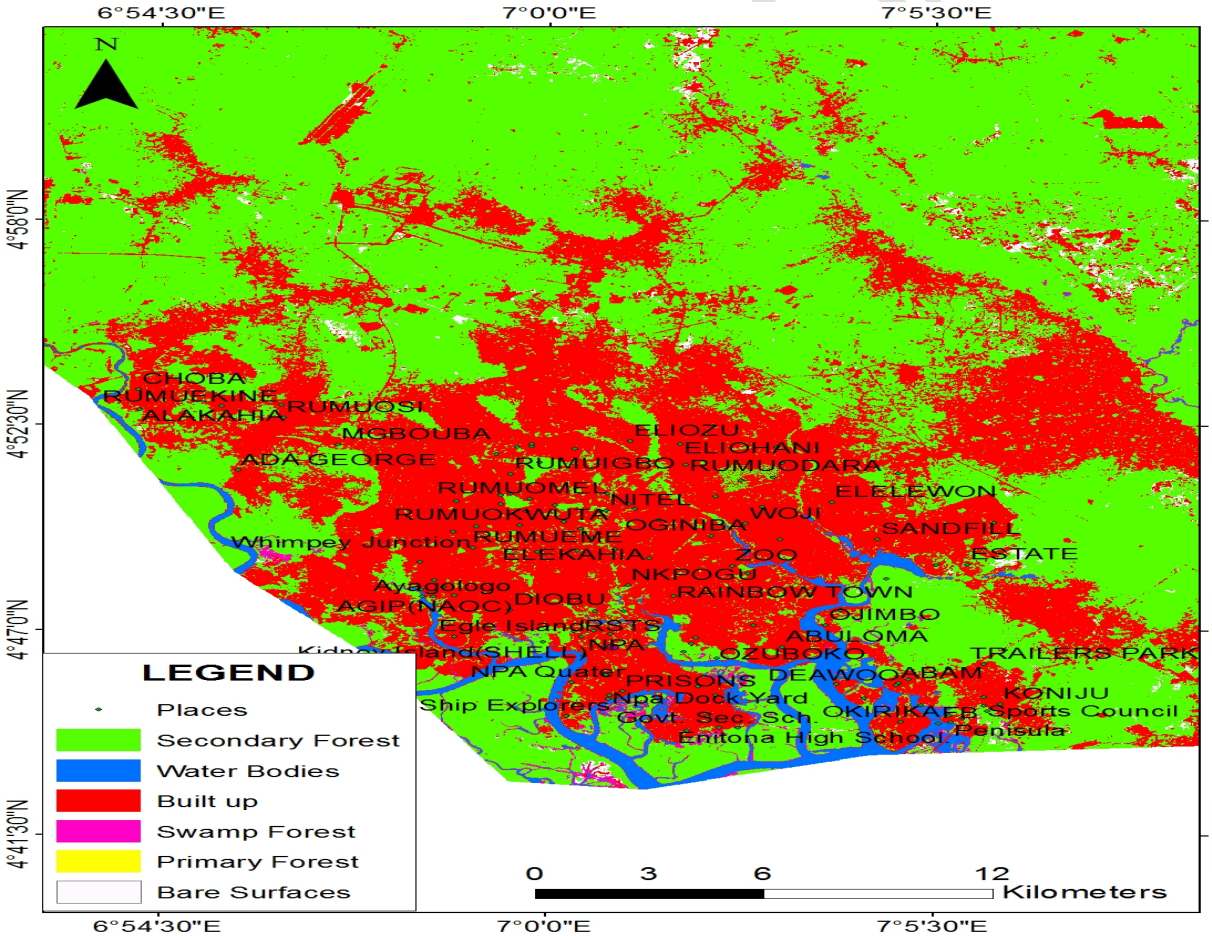

Fig 5 Land Cover of Port Harcourt City and Environs, 2016

213 Table 3: Zone, Land Use Type and Location
214

Zone	Land Use Type	Location
1	Low Residential	GRA, Shell estate, Total estate, Intel zone, Oyibo, Eleme, Igwuruta, Gbolokiri, Etche, Choba, Iwofe, Jetty, Elelenwo, Okirika, Eagle Island, Rumosi, Elekahia, Mgbuoba.
2	High Residential	Diobu, Enitona School Area, D-Line
3	Medium Residential	Ada-George, Abloma, Rumuigbo, Port Harcourt Township, Rumuola, Choba, Mgbuoba, Woji, Okirika, Rumuodara
4	Educational	University of Port Harcourt, University of Science and Technology, Port Harcourt Poly Technique, Ignatious Ajuru University
5	Commercial	Mile One market, Mile 3 Market, Rumuokoro Market, Slaughter, Oil Mill Market, Ikoku market
6	Military	Bori Camp, Airforce, Navy barracks
7	Recreational	Port Harcourt Tourist, Rainbow Zoo, Boro Park, Port Harcourt Pleasure Park, Woji Housing
8	Residential/Commercial	Rumuaghorlu, Rumuokwuta, Rumukrushi, Rumuodomaya, Rumuibekwe, Rukpoku, Orazi, Ogbunabali,
9	Admin/Industrial	Rivers State Secretariat, BMH, UPTH, Transamadi, Agip, Marine Base, NPA, Eleme Petrochemical area.
10	Rural	Elibrada, Aleto, Dankiri, Obeta, Omuagwa as control site

215
216
217
218
219
220
221
222
223
224
225
226
227
228

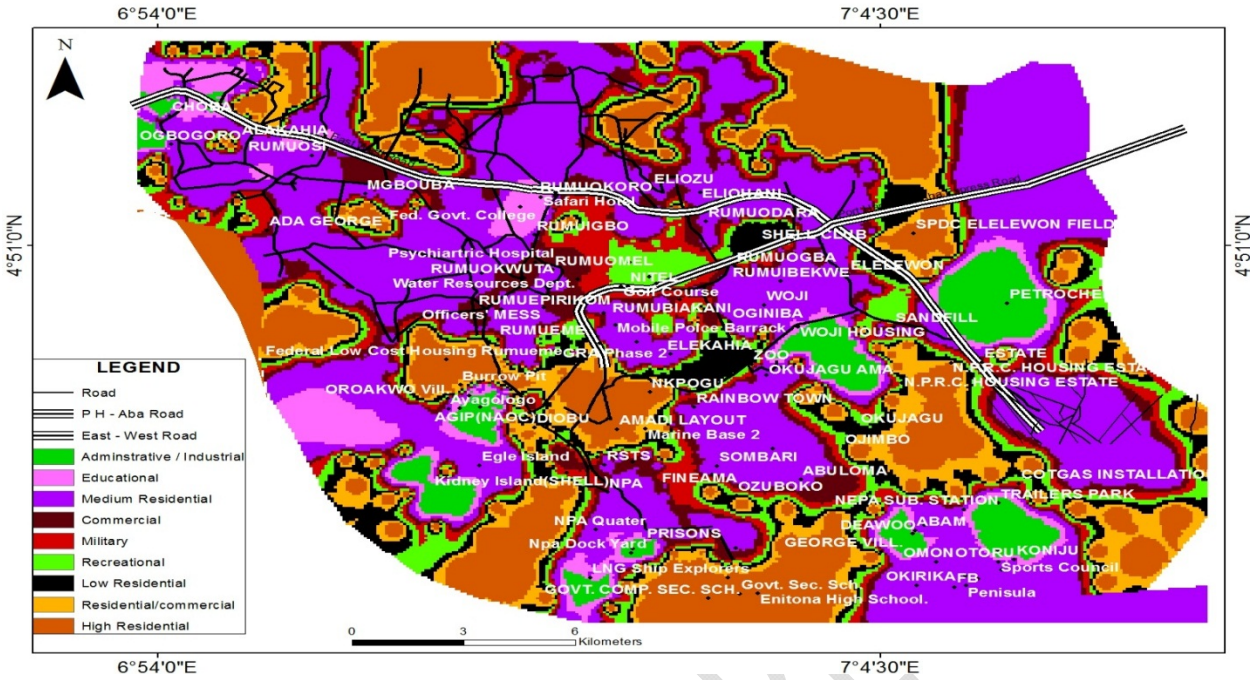

Fig 6 Land Use Types of Port Harcourt City and Environs

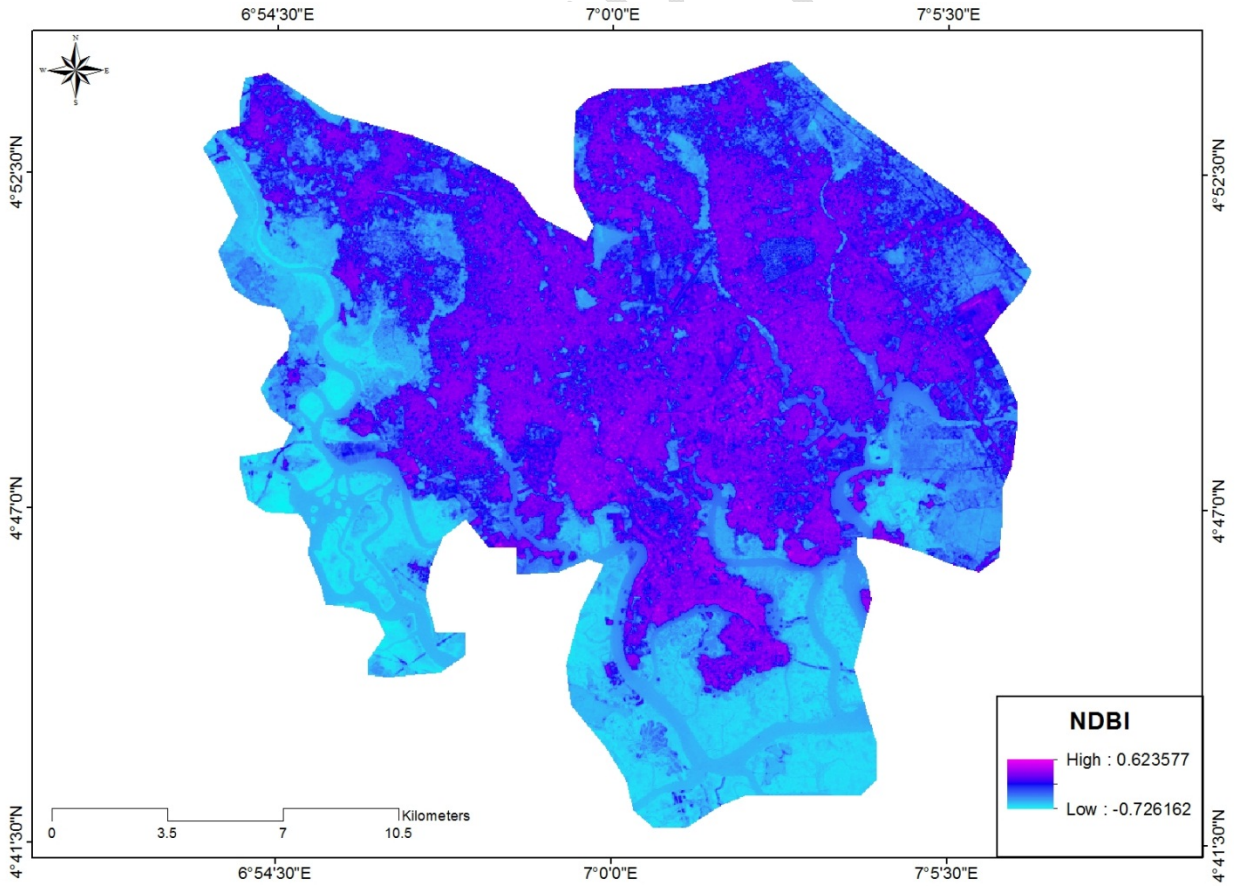

Fig 7 NDBI of Port Harcourt City and Environs (Wet Season)

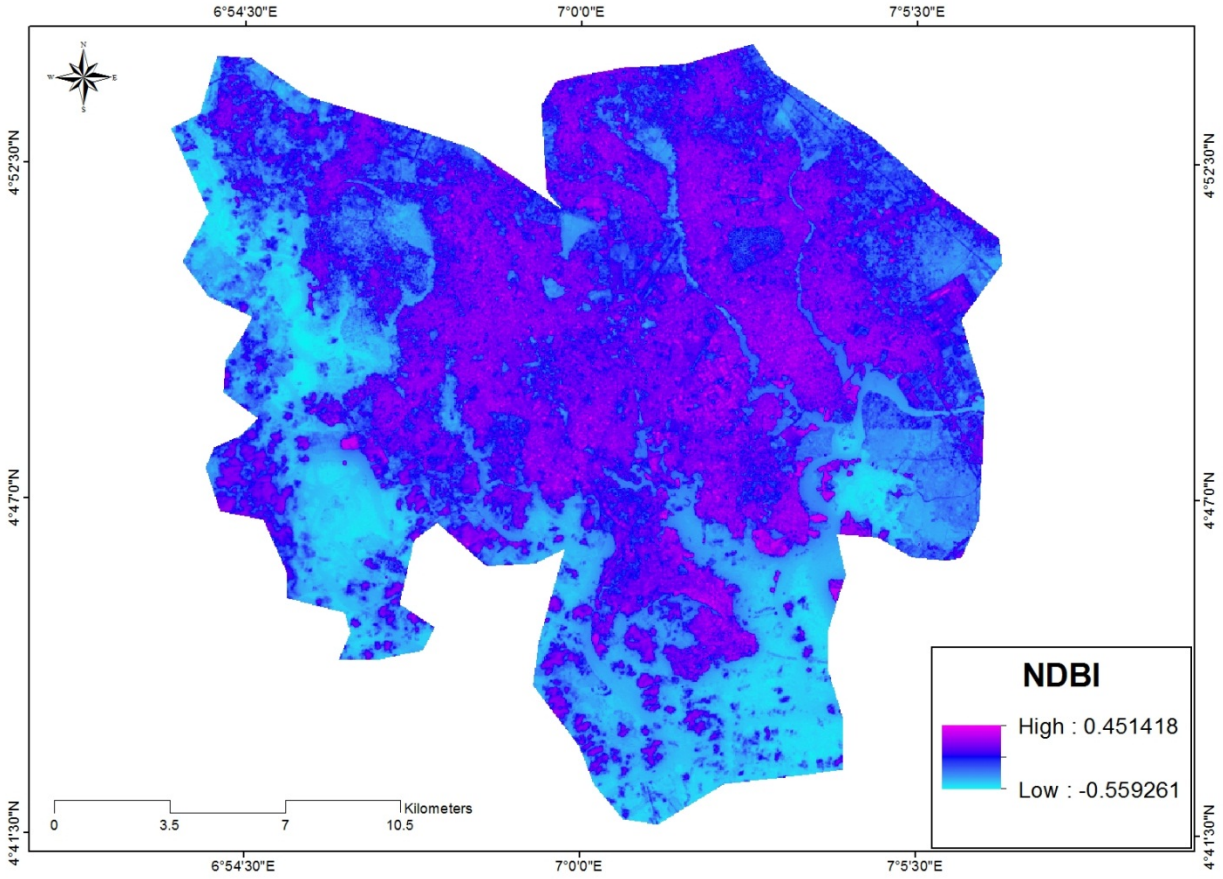

Fig 8 NDBI of Port Harcourt City and Environs (Dry Season)

3.2 SEASONAL VARIABILITY OF LST AND LSE

LST and LSE of Port Harcourt and its metropolis have shown the impact of heterogeneity of surface areas in wet and dry seasons. LST and LSE displayed thermal conductivity of the city surface areas as they affect urban bias and the resultant human discomfort across various land use types from the city center to the rural outskirts. In the wet season (Figure 9), LST concentrated on the city center and spread toward the north-east and north-western part. It extends to surface areas of Choba, Rumuodogo, Elekahia and Rumuekini of the extreme rural fringes in the north-western segment of the city. From the city center to the rural outskirts, LST recorded strong approximate variation of 9.3^0C. LST was limited in the south, south-west and south-eastern parts of the city such as the Kalio Island and Fenema due to intense vegetal cover and water bodies extending to the Atlantic Ocean. Also, LST was scattered on different spots in the city. On the other hand, during the dry season (Figure 10), LST was high at the city center and extends to the center and south-eastern part. It was highly limited in the south, south-west and north-western parts of the city with a variation of approximately 4.8^0C indicating that it was weaker in the dry season. The pattern of LST during the dry season was more of clusters especially at the city center. LST was more intensive in the wet season and weak during the dry season (Figure 11) suspected to be accelerated by heat of evaporation which was mostly pronounced during the wet season due to larger expanse of water surface during the season. Surfaces inside the city have the highest LST. The city center had LST seasonal variation of 11.2^0C, inner city 9.1^0C, medium

8.1^{0}C, outskirts 7.4^{0}C and extremely outskirt 6.7^{0}C across the various city segments. There was strong variation of 9.3^{0}C during the wet season and weak variation of 4.8^{0}C in the dry season contributed by high urban pavement materials and low vegetation at the city center, but high vegetal cover and low pavement materials were found at the rural outskirts indicating that people at the urban outskirts would be more comfortable than those in the inner city. The city center had higher LST value of 32.9^{o}C during the wet season and 21.7^{0}C in the dry season compared to the extreme rural outskirt with 23.6^{0}C wet and 16.9^{0}C dry season respectively.

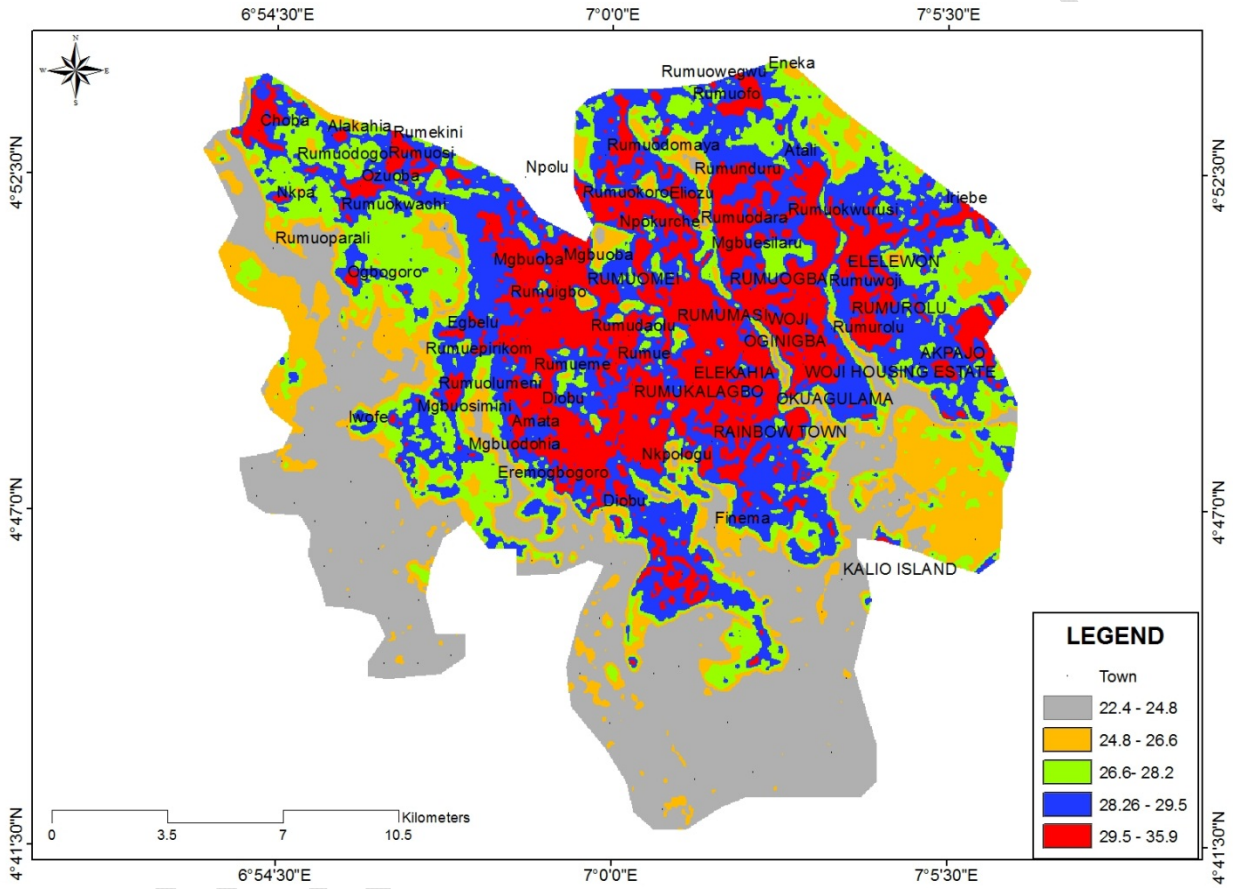

Fig 9 LST of Port Harcourt City and Environs (Wet Season)

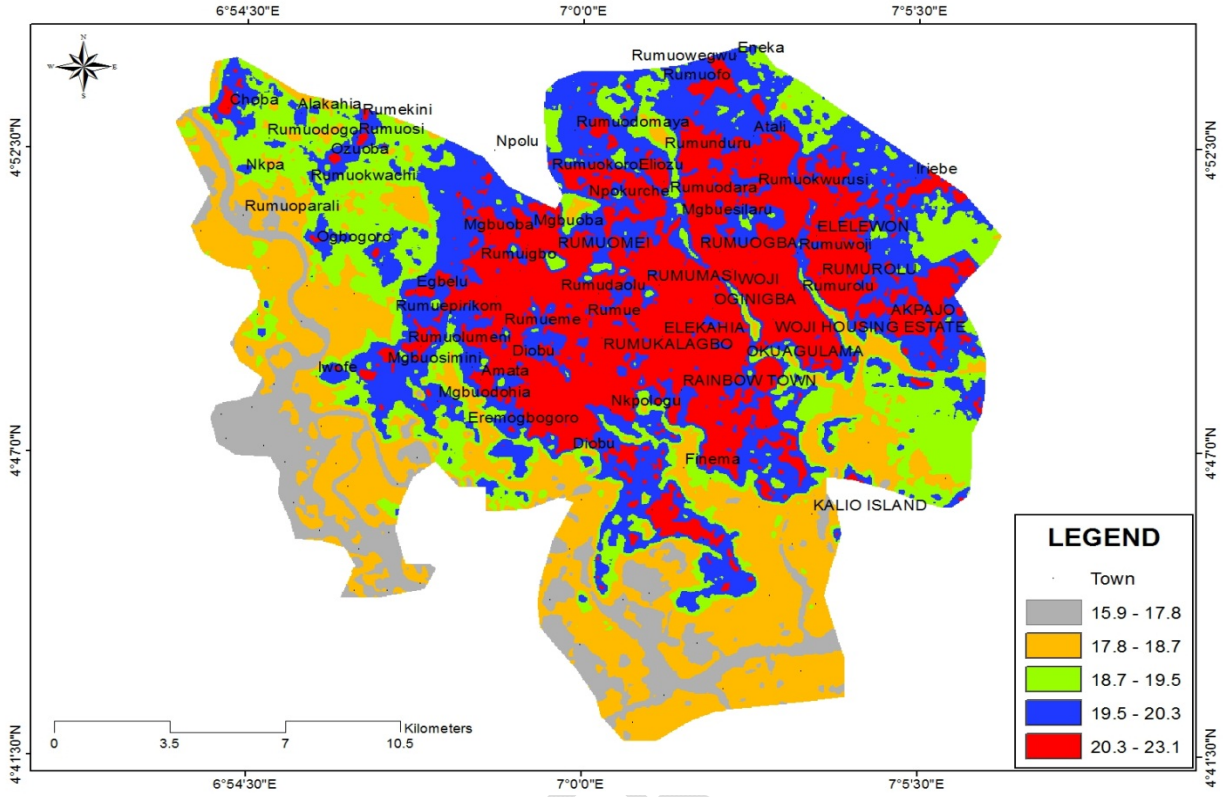

Fig 10 LST of Port Harcourt City and Environs (Dry Season)

	Etremely Outskirt	Outskirt	Medium	Inner City	City Centre
Wet	23.6	25.7	27.4	29.1	32.9
Dry	16.9	18.3	19.6	20	21.7
Difference	6.7	7.4	8.1	9.1	11.2

Fig 11 Comparison of LST of Port Harcourt City and Environs (Wet and Dry Seasons)

Land surface emissivity which is the energy radiated from urban material surfaces per second with the values between 1 (high) and 0 (low). Emissivity in wet season (Figure 12) was distributed in all parts of the city at different intensity. LSE is intensive in the extreme north-west and north-eastern parts seemingly influenced by large area of vegetal cover. LSE was inhibited by large water bodies in the southern part of the city which restricted spread of vegetation and urban materials. On the other hand, LSE in the dry season was pronounced in the southern segment due to reduced water bodies, more coverage of vegetation and exposed urban pavement materials during the season. The extreme north-west and north-eastern parts of the city exhibited high LSE during the dry season. LSE increases from the extreme rural outskirts to the city center (Figure 13) due to high absorption of solar radiation by vegetation and water bodies that store large amounts of heat in the day and gradually release them into the atmosphere. While in the inner city and city center urban pavement materials rapidly absorb solar energy and quickly release energy stored in them in the form of latent heat. Also, surface area in the rural fringes full of vegetation and water bodies has higher emissivity performance. Vegetation and water bodies have more emissivity values than urban materials. This is in tandem with [26] who studied emissivity of crop plants such as mature Phalaenopsis, Paphiopedilum, Malabar and chestnut recording the values of 0.9809, 0.9783, 0.981 and 0.9848 respectively. Sand, water and green grass have emissivity values of 0.949 - 0.962, 0.993 - 0.998 and 0.975 - 0.986 compared to the low emissivity of urban materials such as concretes 0.95-0.97,cement 0.54, gravel 0.28, bricks 0.90-0.94, asbestos 0.96 and aluminum 0.05-0.77 respectively [27]. As a result, the rural fringes have the capacity to emit more solar energy in the form of latent heat to the surrounding atmosphere than the inner city and city center.

In both seasons (Figure 14), LSE rises from the extremely outskirt segment of the city to a peak in the immediate outskirt and drop in the middle part and a sharp rise at the inner city to a fall in the city center. The rise of LST from the beginning of the rural fringes is due large area coverage and increased emissivity due to vegetal cover and water bodies as they have higher emissivity values than urban materials. Low emissivity of the city center area is accelerated by the low emissivity conduction of urban pavement materials, high emissivity performance of vegetal cover and water bodies down the city area. The difference between wet and dry seasons emissivity at the extremely rural outskirts is 0.003, outskirt 0. 0007, medium 0.0004, inner city 0.0024 and city center was 0.001 respectively. Emissivity in the wet season varied with 0.0136 and 0.0006 during the dry season. And both seasons have total emissivity variation of 0.0165. There is thermal radiation exchange between the rural outskirts and the city center usually accelerated by wind velocity. However, LSE decreases from the rural fringes to the city center and LST increases from the rural fringes to the city center due to spatial variation of vegetal cover, water bodies and general urban pavement materials across various segments of the city surface area.

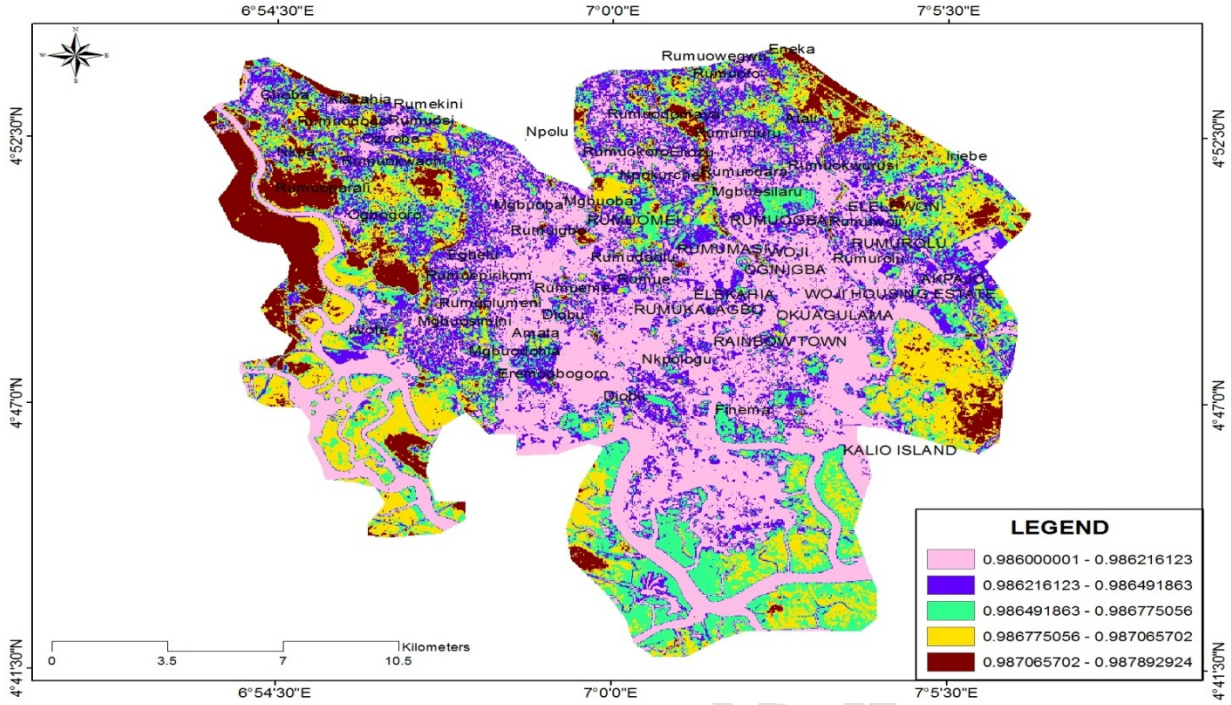

Fig 12 LSE of Port Harcourt City and Environs (Wet Season)

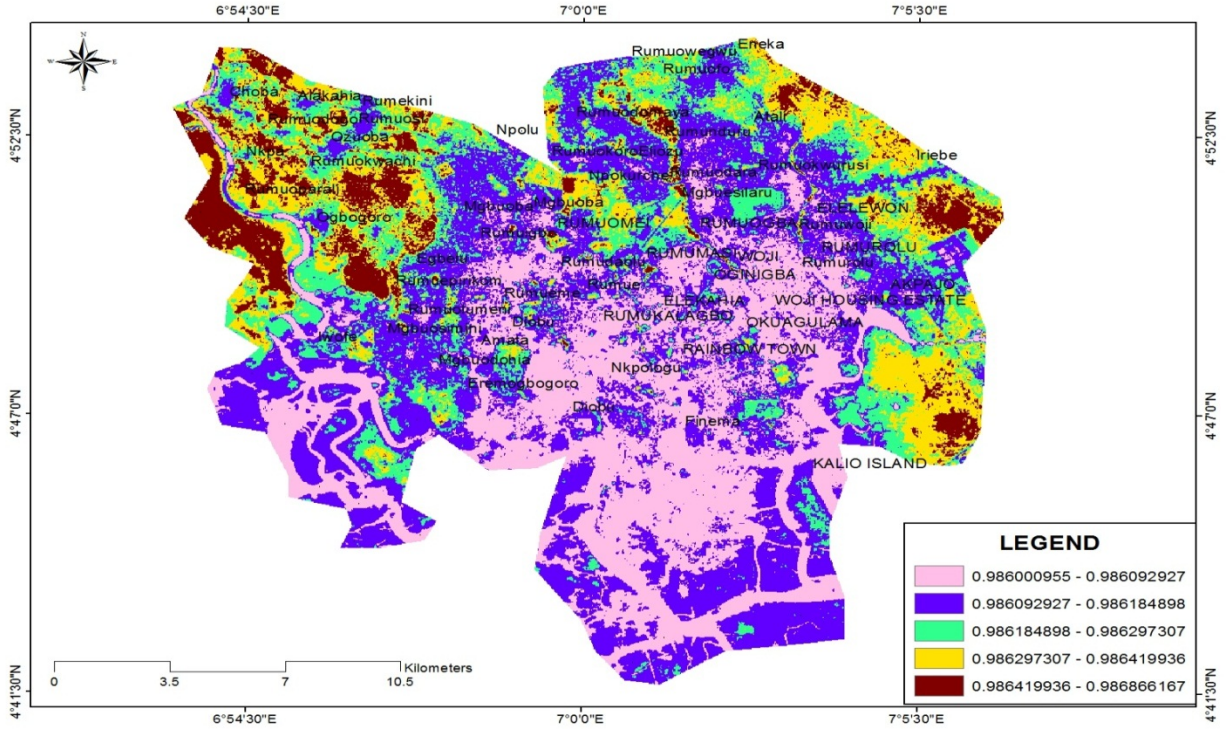

Fig 13 LSE of Port Harcourt City and Environs (Dry Season)

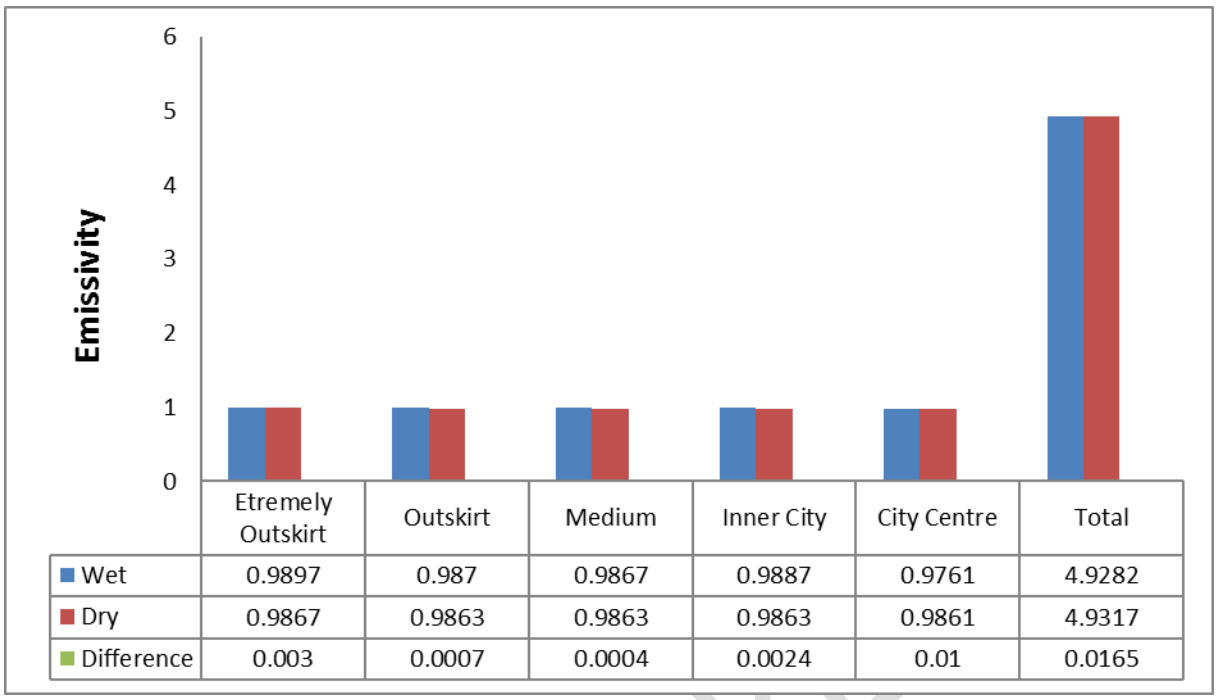

	Etremely Outskirt	Outskirt	Medium	Inner City	City Centre	Total
Wet	0.9897	0.987	0.9867	0.9887	0.9761	4.9282
Dry	0.9867	0.9863	0.9863	0.9863	0.9861	4.9317
Difference	0.003	0.0007	0.0004	0.0024	0.01	0.0165

Fig 14 Comparison of LSE of Port Harcourt City and Environs (Wet and Dry Seasons)

3.2 Conclusion

Investigation was carried out on Land Surface Temperature (LST) and Land Surface Emissivity (LSE) of Port Harcourt City and Environs where satellite remote sensing of multiple-wavelength origin was employed to derive data from the Landsat Enhance Thematic Mapper (ETM+). Statistical mean and range were used for analysis to understand pattern of LST and LSE as they are influenced by land use parameters. The study established the relationship and characteristics of land use land cover, built-up area, LST, LSE and the influence of the growing population on land surface of Port Harcourt and its surrounding rural fringes. With population of over 3,095,342 persons occupying surface area of approximately 458,28Km^2, rapid vegetal and water body lost have put the city area under pressure of 4.7^{0}C heat bias within 15 year interval. As a result, LST and LSE indicate that the surface thermal conductivity of the city varied from the extreme rural outskirts to the city center in both wet and dry seasons. LST spread from the city center to the northern part and limited in the southern part due to constraints of water bodies and forest vegetation. Generally, LST differ from the rural segment to the city center with 9.3^{0}C during the wet season and 4.8^{0}C in the dry season respectively indicating weak surface temperature during dry season due to differential heat of evaporation. LSE is severe in the southern part of the city contributed by water bodies, more vegetal cover and urban pavement materials during the dry season. And LSE in the wet season is intensive in the extreme north-west and north-eastern parts influenced by large area of vegetation and water bodies. It is recognized that vegetation and water bodies have higher emissivity values than urban manmade materials making the rural fringes have more emissivity coefficient compared to the city center. Thus, emissivity rises from the rural

environment and drops at the city center. Emissivity in the wet season varied with 0.0136 and 0.0006 during the dry season. LSE varied in wet and dry seasons with 0.0165 radiation value. However, one critical finding is that LSE decreases from the rural fringes to the city center and LST increases from the rural fringes to the city center due to spatial variation of vegetal cover, water bodies and general urban pavement materials across various segments of the city surface areas. It is therefore, recommended that urban land use management should be improved in the city, urban greening at the city center should be practiced and the rural fringes should be explored by decongesting activities at the city center and controlled with policy implementation to reduce heat bias in Port Harcourt coastal city of tropical Africa.

REFERENCES

[1] Kjellstrom, T.; McMichael, A.J. (2013). Climate change threats to population health and well-being: The imperative of protective solution that will last. Glob. Health Action, 6, (pp 1–9).

[2] Balogun, A. A., Balogun, I. A., Adefisan, A. E. and Abatan, A. A. (2009). Observed characteristics of the urban heat island during the harmattan and monsoon in Akure, Nigeria. Eight Conferences on the Urban Environment. AMS 89th Annual Meeting, 11 – 15 January, Phoenix, AZ. Paper JP4.6. http://ams.confex.com/ams/pdf papers/152809.pdf. Accessed 19 February 2018

[3] Kotani, A. and Sugita, M. (2005). Seasonal variation of surface fluxes and scalar roughness of suburban land covers. Journal of Agricultural and Forest Meteorology. (135), 1–21.

[4] Santamouris, M. (2001). The role of green spaces. Energy and climate in the urban built environment, (pp 145-159).

[5] Yamashita, S. (1996). Detailed structure of heat island phenomena from moving observations from electric tram-cars in metropolitan Tokyo. Atmos. Environ. 30, 429–435.

[6] Rao, P.K. (1972). Remote sensing of urban heat islands from an environmental satellite. Bull. Am. Meteorol. Soc. 53, 647–648.

[7] Zhao, J and Wang, N. (2002). Remote Sensing analysis of urbanization effect on climate in Lanzhou. Arid Land Geography, 25(1), 90-95.

[8] Gluch, R.; Quattrochi, D.A. (2006). Luvall, J.C. A multi-scale approach to urban thermal analysis. Remote Sens. Environ. 104, 123–132.

[9] Weng, Q.; Liu, H.; Liang, B.; Lu, D. (2008). The spatial variations of urban land surface temperatures: Pertinent factors, zoning effect, and seasonal variability. IEEE J. Sel. Top. Appl. Earth Obs. Remote Sens. 1, 154–166.

[10] Kerr, Y. H., Lagouarde, J. P., Nerry, F., and Ottlé, C. (2000). Land surface temperature retrieval techniques and applications. In D. A. Quattrochi, & J. C. Luvall (Eds.), Thermal remote sensing in land surface processes (pp. 33–109). Boca Raton, Fla.: CRC Press.

[11] Xiao, R.; Weng, Q.; Ouyang, Z.; Li,W.; Schienke, E.W.; Zhang, Z. (2008). Land surface temperature variation and major factors in Beijing, China. Photogramm. Eng. Remote Sens, 74, 451.

[12] Peres, L. F. and DaCamara, C. C. (2004). Land surface temperature and emissivity estimation based on the two-temperature method: sensitivity analysis using simulated MSG/SEVIRI data. Remote Sensing of Environment, 91, 377–389.

[13] Chen, L. F., Zhuang, J. L., Xu, X. R., Niu, Z., Zhang, R. H., & Xiang, Y. Q. (2000). The definition and validation of nonisothermal surface's effective emissivity. Chinese Science Bulletin, 45(1), 22-29.

[14] Weibo, L., Johannes, F., Leiqiu, H., Ashley, Z. and Nathaniel, B. (2017). Seasonal and Diurnal Characteristics of Land Surface Temperature and Major Explanatory Factors in Harris County, Texas. Sustainability, 9, 2324. doi:10.3390/su9122324.

[15] Chiadikobi, K.C., Omoboriowo, A.O., Chiaghanam, O. I., Opatola, A. O. and Oyebanji, O. (2011). Flood Risk Assessment of Port Harcourt, Rivers State, Nigeria. *Advances in Applied Science Research.* 2(6), 287-298.

[16] Fasote, J. (2007). Assessment of land-use and land-cover changes in Port Harcourt and Obio/Akpor local government areas using remote sensing and GIS approach.

[17] Odu, N. N. and Imaku, L. N. (2013). Assessment of the Microbiological Quality of Street-vended Ready-To-Eat Bole (roasted plantain) Fish (*Trachurustrachurus*) in Port Harcourt Metropolis, Nigeria. *Researcher,* 5(3): 9-18.

[18] Figueroa, P. I. and Mazzeo, N. A. (1998). Urban-Rural Temperature Differences in Buenos Aires. *International Journal of Climatology*, 18, 1709-1723.

[19] Edokpa, D. O. and Nwagbara, M. O. (2017). Atmospheric Stability Pattern over Port Harcourt, Nigeria. *Journal of Atmospheric Pollution*, 5(1), 9-17.

[20] Mmom, P. C. and Fred-Nwagwu, F.W. Analysis of Land use and Land cover Change around the City of Port Harcourt, Nigeria. 2013.

[21] Utang, P.B. and Wilcox, R.I. (2009). Applying the Degree Days Concept in indicating Energy Demand due to climate change in Port Harcourt, Nigeria. Port Harcourt *Journal of Social Science,* 1(2), 89-102.

[22] Qin, Z., Karnieli, A. and Berliner, P. (2001). A Mono-Window Algorithm for Retrieving Land Surface Temperature from Landsat TM Data and Its Application to the Israel-Egypt Border Region. *International Journal of Remote Sensing*, 18, 3719-3746. :doi.org/10.1080/01431160010006971.

[23] Oke, T.R. City Size and the Urban Heat Island. *Atmospheric Environment,* l7, 769-779.1973.

[24] National Population Commission. (2006). https://www.google.com.ng/?gfe_rd=cr&ei=Kqn2WMOOBrGn8weazqO4CA&gws_rd=ssl#q=2006+national+population+census. Accessed 19 February 2018.

[25] Olatunde, S. E. and Olalekan, A. (2015). Spatio-temporal Analysis of Wetland change in Port- Harcourt Metropolis. Tanz. J. Sci. 41.

[26] Robert Hadfield (2005). Determining the Leaf Emissivity of Three Crops by Infrared Thermometry. doi:10.3390/s150511387.

[27] Emissivity Table. 2018. https://thermometer.co.uk/img/documents/emissivity_table.pdf. Accessed 26 April 2018.